Computers & Geosciences 37 (2011) 1067–1074

Contents lists available at ScienceDirect

Computers & Geosciences

journal homepage: www.elsevier.com/locate/cageo

Surface Lagrangian Remeshing: A new tool for studying long term evolution of continental lithosphere from 2D numerical modelling

Philippe Steer [a,b,*], Rodolphe Cattin [a], Jérôme Lavé [c], Vincent Godard [d]

[a] Géosciences Montpellier, CNRS-UMR 5243, Université Montpellier 2, 34000 Montpellier, France
[b] Laboratoire de Géologie, CNRS-UMR 8538, Ecole Normale Supérieure, 75005 Paris, France
[c] CRPG, CNRS-UPR2300, 54501 Vandœuvre-lès-Nancy, France
[d] CEREGE, CNRS-UMR 6635, Aix-Marseille Université, 13545 Aix-en-Provence, France

ARTICLE INFO

Article history:
Received 14 February 2010
Received in revised form
27 May 2010
Accepted 29 May 2010
Available online 4 November 2010

Keywords:
Local remeshing
Numerical model
Finite element
Erosion

ABSTRACT

In this paper we present a new local remeshing algorithm that is dedicated to the problem of erosion in finite element models whose grid follows the movement of the free surface. The method, which we name Surface Lagrangian Remeshing (SLR), is adapted to 2D Lagrangian models which couple surface erosion with deformation of Earth materials. The remeshing procedure preserves nodes defining the surface submitted to erosion and removes nodes belonging to surface elements whose internal angles or area is critically low. This algorithm is ideally suited to track long term surface evolution. To validate the method we perform a set of numerical tests, using triangular finite elements, which compare the results obtained with the SLR algorithm with global remeshing and with analytical results. The results show good agreements with analytical solutions. Interpolation errors associated with remeshing are generated locally and numerical diffusion is restricted to the remeshed domain itself. In addition this method is computationally costless compared to classical global remeshing algorithm. We propose to couple the SLR method with the Dynamical Lagrangian Remeshing (DLR) algorithm to enable local remeshing only of Lagrangian models coupling large deformation of Earth materials with large erosion.

1. Introduction

Over the last two decades studies based on numerical modelling have demonstrated that the interaction of surface erosion and deformation of continental lithosphere is a key process in orogenic evolution (e.g., Avouac and Burov, 1996; Beaumont et al., 1992; Godard et al., 2009; Willett, 1999). These numerical approaches are commonly based on both an erosion law controlling the evolution of surface topography and a thermo-mechanical finite element model (FEM) that accounts for lithospheric deformation. However, as previously mentioned (e.g., Kurfeß and Heidbach, 2009) the major limitation of coupled models is that the FEM based on a Lagrangian formulation cannot perform simulations over very long time scales, due to the development of large cumulative deformation. Finite element methods are based on the spatial discretization of tensor and scalar values onto a finite number of elements. In the Lagrangian formulation the shape and location of these elements evolve with the deformation within the model together with erosion processes at the top surface. The quality of the numerical solution is closely linked to the shape functions used to interpolate discrete node quantities into continuous field variables. Shape functions are geometrically defined and as a consequence cumulated deformation of elements over long time scales leads to a decrease in the quality of interpolation.

To overcome this major limitation most of the numerical approaches use remeshing algorithms to work on undistorted and well focused mesh. Remeshing is then associated with transfer of parameter fields between two subsequent meshes. This requires interpolation, which is a common source of numerical diffusion. In geosciences remeshing is commonly used for the study of crack propagation (e.g., Belytschko and Black, 1999), flow description (e.g., Hwang and Wu, 1992) or long-time scale lithospheric deformation (e.g., Godard et al., 2009; Yamato et al., 2007). Most of these algorithms perform global remeshing, which requires transferring the field variables over the entire model.

To reduce numerical diffusion associated with the remeshing procedure many numerical strategies have been developed. For example Yamato et al. (2007) use an array of additional passive markers to interpolate field variables. Fullsack (1995) has developed a FEM based on the arbitrary Lagrangian–Eulerian (ALE) formulation. In this formulation the finite element calculation is

* Corresponding author at: Géosciences Montpellier, CNRS-UMR 5243, Université Montpellier 2, 34000 Montpellier, France. Tel.: +33 4 67 14 41 56; fax: +33 4 67 14 36 42.
E-mail addresses: philippe.steer@gm.univ-montp2.fr (P. Steer), cattin@gm.univ-montp2.fr (R. Cattin), jlave@crpg.cnrs-nancy.fr (J. Lavé), godard@cerege.fr (V. Godard).

0098-3004/$ - see front matter © 2010 Elsevier Ltd. All rights reserved.
doi:10.1016/j.cageo.2010.05.023

not performed on the tracking mesh (a Lagrangian one) but rather on an Eulerian one. Even if those methods (passive markers and ALE) are efficient to reduce interpolation errors, they lead to expensive CPU time-cost or require large amounts of memory. Yet note that ALE methods can be enhanced by the use of adaptative grid based on an octree division of space, which enables to interpolate field variables only for the appropriate elements (Braun et al., 2008; Thieulot et al., 2008).

An alternative approach is local remeshing algorithms, where only the distorted elements and their neighbours are remeshed. The additional benefit of these algorithms are that they reduce CPU time cost associated with remeshing. Braun and Sambridge (1994) propose the local Dynamical Lagrangian Remeshing (DLR) algorithm to deal with the distortion of the triangular elements of Lagrangian FEM. This method is suited to address high deformation problems. However, it is not adapted to numerical modelling with intense erosion, in which mass removal by erosion not only affects the surface elements shape but also reduces their area.

In this paper, using the lagrangian FEM code ADELI (Hassani et al., 1997) we propose a complementary approach called Surface Lagrangian Remeshing (SLR hereinafter) algorithm to deal with the distortion and area decrease of surface elements by erosion. In what follows after a detailed presentation and tests of the SLR method, we will focus on the application of this method to study classical surface erosion laws. Coupled with the DLR method this local remeshing technique can be applied to investigate a wide set of geodynamical problems including interactions between deformation and erosion.

2. Local remeshing algorithms

2.1. Coupling erosion and deformation: remeshing approach

Compared to global remeshing, local remeshing only modifies a small area close to the distorted elements. The Dynamical Lagrangian Remeshing (DLR) algorithm (Braun and Sambridge, 1994) was developed to deal with distortion by deformation of the triangular elements of Lagrangian FEM. DLR consists in a permanent reconnection of nodes with their closer neighbours by a Delaunay triangulation (Fig. 1). It forces elements to respect the Delaunay condition on the grid: the strict interior of the circumcircle of each triangular element contains no node. As previously mentioned this method is very efficient to model high deformation problems, but it cannot be applied to remesh surface elements affected by erosion. Here we propose the SLR method as a complementary algorithm to the DLR method and dedicated to surface erosion. In depth the DLR algorithm deals with the remeshing of highly deformed non-Delaunay elements (see Fig. 1 bottom image) whereas the SLR algorithm enables to keep unflatened elements at surface (see Fig. 1 top image). From now on we focus only our study on the SLR method. We refer the reader to Braun and Sambridge (1994) for further details on the DLR method.

2.2. Surface Lagrangian Remeshing (SLR) algorithm

The main difficulty which must be solved by the SLR method consists in the local remeshing of deformed surface elements without altering the topographic profile itself. This latter is a critically important feature of the models investigating coupling between surface processes and tectonics. Thus, in the SLR algorithm only the internal nodes, i.e. the nodes that do not belong to the surface, are concerned by remeshing.

In our approach we use triangular elements initially generated by the Delaunay triangulation. We define the critical elements in respect to remeshing, as the elements which exhibit at least one small internal angle $\alpha_{int} < \alpha_{cri}$ or a small area $A/A_{ini} < A_{cri}$. Two geometrical conditions apply on the critical angle α_{cri}: (1) $\tan(\alpha_{cri})$ must be greater than the ratio of the maximum erosion Δh_{max} during one time step, over the minimum vertical height of the surface elements h_{min},

$$\tan(\alpha_{cri}) > \Delta h_{max}/h_{min}. \quad (1)$$

(2) α_{cri} must be smaller than 25° to avoid mesh destruction. The critical area A_{cri} is a secondary criterion, which preserves the simulations from both frequent remeshing and major area decrease of surface elements. In the following the critical angle α_{cri} and area A_{cri} are set to 18° and 50% of the initial area, respectively.

The SLR method is applied to the top surface of the model and consists of three stages: (1) internal nodes sharing at least one connection with surface nodes and belonging to critical elements are removed from the mesh. (2) Next, critical elements and their

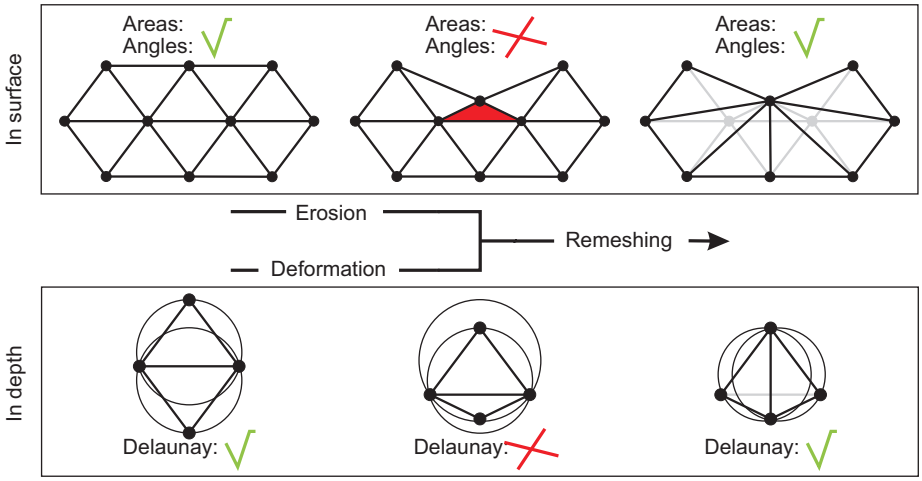

Fig. 1. Description of the geometric principle of the SLR (top) and DLR (bottom) methods (Braun and Sambridge, 1994). Top image: the initial mesh is eroded until at least one angle or one area of a triangular element of the surface becomes critical; after erosion, the area A of the filled triangle is critical, compared to its initial value A_i, $A/A_i < A_c$, where $A_c = 0.5$ is the critical area ratio. A remeshing criterion on the internal angles of the surface triangles is also defined. A triangle with at least one internal angle below 18° becomes critical. Nodes of the critical triangle, which are not at surface, are removed from the mesh. Triangles that include these removed nodes are deleted. Remaining nodes are reconnected by a Delaunay triangulation algorithm. After remeshing, the old mesh is indicated by gray lines. Bottom image: the initial mesh is deformed in depth until the Delaunay condition becomes false, i.e. the strict interior of the circumcircle of each triangular element contains no node. After reconnection of these nodes to their closest neighbours, the Delaunay condition becomes true again.

direct neighbours are also deleted from the mesh and replaced by new triangular elements following a Delaunay triangulation algorithm (Renka, 1996). (3) Finally, tensor and scalar values defined by elements are interpolated from the old to the new mesh. We use a simple conservative interpolation scheme, in which each new element value V_{new} is equal to the spatial integral of the old elements value V_{old} on the new element domain Ω divided by the area of Ω,

$$V_{new} = \frac{\int_{\Omega} V_{old}(\omega)\, d\omega}{\int_{\Omega} d\omega}, \quad (2)$$

where $d\omega$ is an infinitesimal area.

The SLR algorithm presents three main advantages: (1) by remeshing only critical and highly deformed surface elements, SLR method generates numerical errors only on the local remeshed domain. (2) Nodal values are not interpolated during remeshing as there is no redistribution of nodes position during remeshing. (3) The combination of nodes defining the surface is kept constant and thus it does not artificially introduce any surface profile change, which would be a major drawback when considering geomorphological issues.

3. Validation of the SLR method

3.1. SLR and tracking of the surface

To check the ability of the SLR method to preserve surface profile during remeshing, simple models of erosion using SLR are compared with corresponding analytical solutions (Fig. 2). The numerical solutions are obtained with the FEM code ADELI (Hassani et al., 1997). These experiments of comparison consist in eroding completely, until peneplanation at $t = t_{\star}$, a triangular-shaped mountain with a basal width of 100 km and a summit height of 3 km lying over a rigid and incompressible medium. The top surface is subjected to different erosion laws: erosion by diffusion of elevation $\partial h/\partial t = K\partial^2 h/\partial x^2$ (Avouac and Burov, 1996) or erosion proportional to slope $\partial h/\partial t = K\partial h/\partial x$ (Beaumont et al., 2001), where K is the coefficient of diffusion and a coefficient of denudation, respectively. Analytical solutions are given in Appendix A.

In both cases the numerical results obtained with the SLR method are in very good agreements with the analytical solutions (to the order of 1 cm compared to 3 km of cumulated erosion, see Fig. 2) while $\sim$200 remeshings were performed in each experiment. However, in the slope-dependent erosion law, the numerical solution progressively diverges from the analytical one at the foot of the mountain where the topographic slope varies abruptly. This is due to diffusion of the numerical solution, which is inherent to the upwind-differencing numerical scheme used for numerically solving the surface slope. In these two experiments, the $\sim$200 SLR phases, which were necessary to reach peneplanation, have not significantly altered the evolution of the surface.

3.2. Comparison between SLR and global remeshing

To further quantify the robustness of the SLR method, we perform a set of tests, which compare the results obtained with SLR and a global remeshing method using the same interpolation scheme. The set-up of the model (Fig. 3) used here is similar to the previous one, apart from the rheology which is elastic and is defined by a Young modulus, $E=40$ GPa and Poisson's ratio $\nu = 0.25$. Each component of the elastic strain ε_{ij} is a function of the stress tensor $\boldsymbol{\sigma}$, through Hooke's law,

$$\varepsilon_{ij} = \frac{1+\nu}{E}\sigma_{ij} - \frac{\nu}{E}\mathrm{trace}\,(\boldsymbol{\sigma})\delta_{ij}. \quad (3)$$

The boundaries of the model are fixed except the top surface which is subjected to a more realistic erosion law and follows a classical shear-stress fluvial incision law (Gilbert, 1877; Howard and Kerby, 1983; Howard et al., 1994; Lavé and Avouac, 2001). This approach is not fully compatible with mechanical modeling, which requires to consider mean elevation as the pertinent upper boundary variable (Godard et al., 2006). We refer the reader to Lavé (2005) and Willett (2010) for further details on how to incorporate erosion in geodynamic models.

Time evolution of the river elevation h is expressed as follow:

$$\partial h/\partial t = KP^{\gamma}A^{\beta}(\partial h/\partial x)^{\alpha}, \quad (4)$$

where K is a coefficient related to bedrock erodibility, P the mean precipitation rate of the watershed considered, A the watershed area and α, β, γ, some exponents, set equal to 0.7, 0.27 and 0.33, respectively (Godard et al., 2006; Lavé and Avouac, 2001). Area is deduced from Hack's law, $A = k_a L^h$, where L is the length of the river, k_a and h two empirical constants (Hack, 1957). The bedrock erodibility and precipitation rate are set to $K = 6.4 \times 10^{-10}\ \mathrm{m}^{0.13}\,\mathrm{s}^{-0.67}$ and to $P = 1\ \mathrm{m\,a}^{-1}$, respectively. The model lasts 10 Ma with 10^4 time steps. This setting enables a complete peneplanation of the topography after $\sim$6 Ma.

The final stage of these numerical experiments (peneplanation) is compared to the state of strain of an unremeshed reference model, for which erosion is simulated by an instantaneous removal of the mountain load whit no remeshing. As the plate is purely elastic there should be no difference between this modelling and the global or local remeshed numerical experiments with progressive erosion.

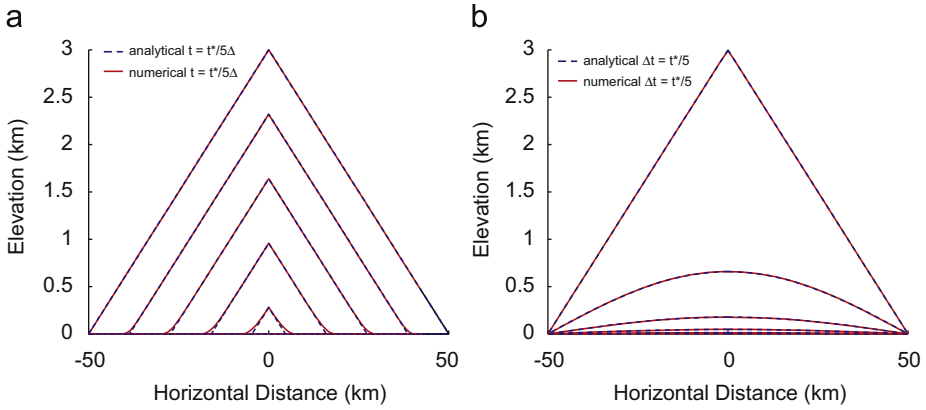

Fig. 2. Time evolution of the surface of the model for different erosion laws plotted at each 20% ($\Delta t = t_{\star}/5$) of the numerical experiment: (a) erosion proportional to slope with $K = 4.0 \times 10^{-10}\ \mathrm{m\,s}^{-1}$ and (b) erosion by diffusion with $K = 3.0 \times 10^{-5}\ \mathrm{m}^2\,\mathrm{s}^{-1}$. Results from these numerical experiments are compared with the corresponding analytical solution. Note that in (b) only the erosive component of the diffusion law is simulated.

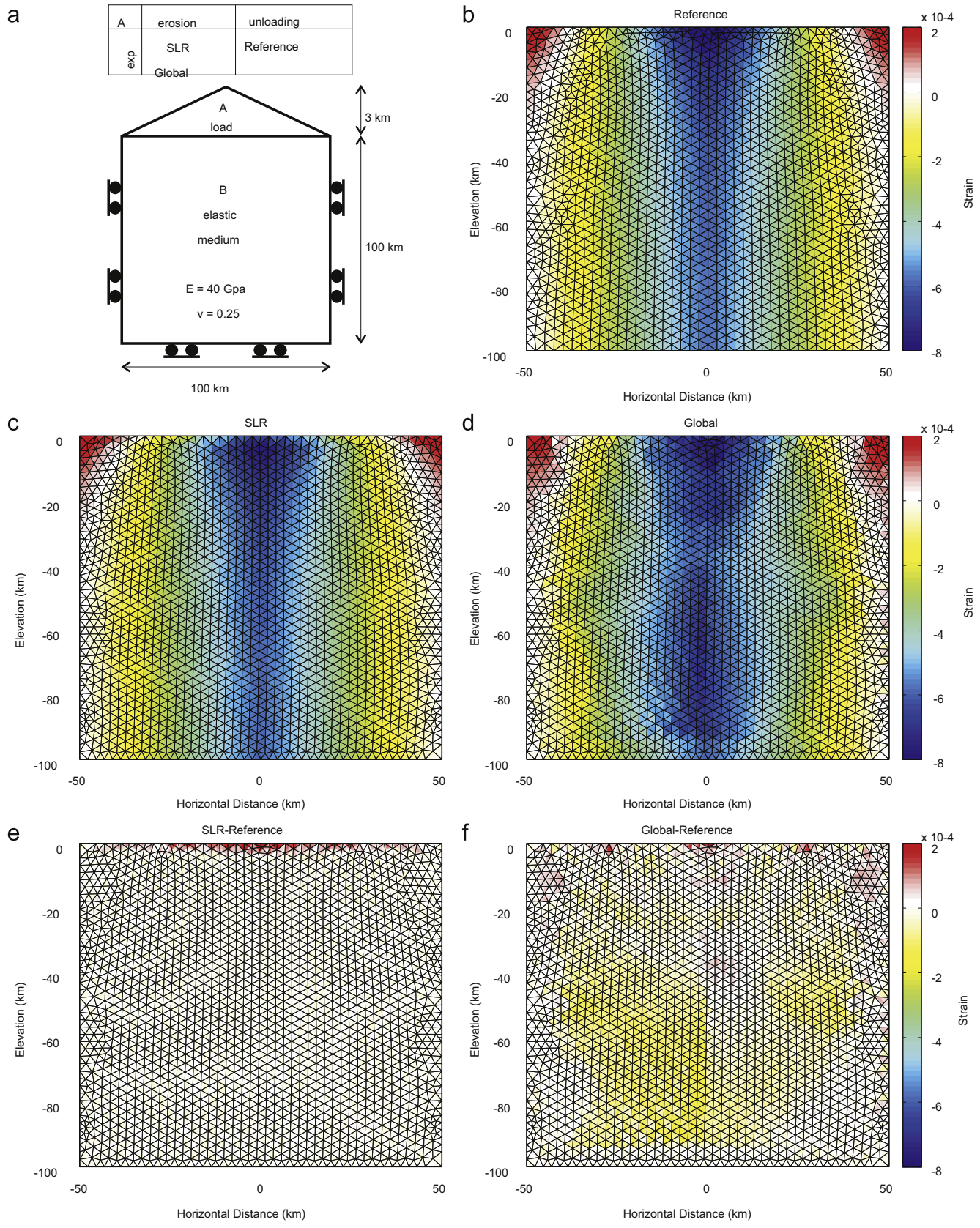

Fig. 3. Results of the numerical experiments comparing local and global remeshing with the reference one. (a) Set-up of the different experiments. The medium A is submitted either to erosion (SLR, Global) or to instantaneous removal (Reference), while the elastic medium B boundary conditions remain constant in the different experiments. The model counts approximatively 6000 elements. Bulk strain field obtained at 10 Ma for the reference model (b), with the Surface Lagrangian Remeshing (SLR) algorithm (c) and with global remeshing (d). Also are represented the differences of the bulk strain field between (e) the SLR experiment and the reference one, and between (f) the Global and the reference ones. Note that SLR produces errors localized only at the surface of the model, while errors produced by global remeshing are wide spreaded across the simulation domain.

In a first approximation both approaches using global and local remeshing algorithms give concordant results showing a localized deformation zone at depth bellow the initially high elevated area (Fig. 3). However, a more detailed analysis of the strain pattern and a comparison with the reference model results reveal some major differences including a zone of intense deformation ($< -6 \times 10^{-4}$) at 50–90 km depth obtained in the global remeshed experiment only. The results obtained with the SLR method appear to be significantly closer to the reference model, apart from the top surface where repetitive local remeshing has lead to numerical errors. This illustrates the role of the remeshed domain size: global remeshing interpolate tensor and scalar values defined by elements over the entire model, while SLR interpolate these values only in the remeshed area. Thus SLR prevents the development of widespread numerical diffusion that is inherent to global remeshing methods.

By producing numerical errors, remeshing can affect the stability of the simulation. Here we use the FEM code ADELI which uses an iterative explicit approach and solves Newton's second law to obtain the static solution of a steady-state modelling (see a detailed description in Appendix B). The convergence of the algorithm is thus associated with the minimization of unbalanced forces (Eq. (16)), which can be expressed through the inertial ratio,

$$I_r = \frac{\|F_e + F_i\|}{\|F_e\| + \|F_i\|}, \tag{5}$$

where F_e and F_i are the external and internal nodal forces acting on the system, respectively. This parameter can thus be used as a proxy of the numerical stability during an experiment: a decrease (increase) of I_r can be associated to a numerical stability increase (decrease) with time.

For both methods (SLR and global remeshing) we obtain an increase in numerical stability with time affected by large pulses of I_r increase associated with remeshing phases (Fig. 4). Our results suggest (1) a lower destabilisation effect due to the SLR method: the inertial ratio exhibits peaks of twice higher amplitude during global remeshing than during SLR and (2) a more frequent remeshing with the SLR method: only six global remeshing are needed when 44 SLR are required. These two features can be easily explained by the differences between the two remeshing methods. Global remeshing, contrary to SLR, completely reorganizes the distribution of nodes and in particular those close to the surface. This enables to space out the remeshing phases, but increases the numerical diffusion, due to interpolation on a greater amount of elements.

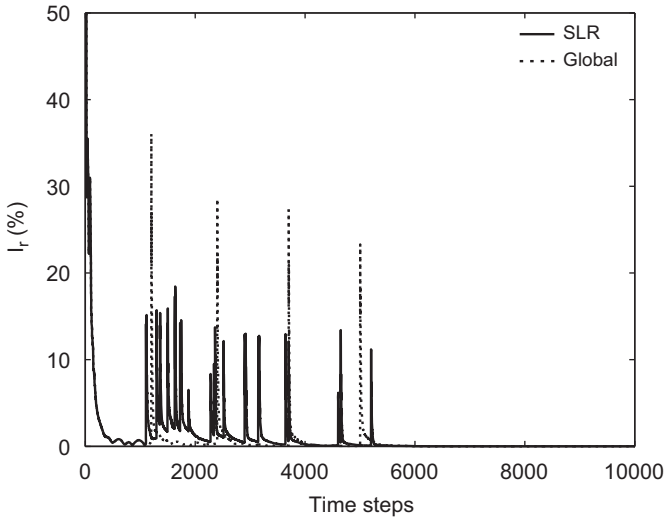

Fig. 4. Evolution of the inertial ratio I_r for the SLR method (bold line) and for the global remeshing method (dashed line).

3.3. Remeshing and computational cost

In the previous experiments our model is meshed with ~6000 elements. The cumulated CPU time for the remeshing and subsequent interpolation is ~1.0 s, while it is equal to ~400 s for global remeshing.

To test the efficiency of the SLR method in a more general way we compare the CPU time associated with local and global remeshing for models with a number of elements between 500 and 20 000 (Fig. 5). Our results show that the CPU time for each remeshing phase increases proportionally as the square of the number of elements for global remeshing, whereas it is almost constant for SLR. Accurate simulations require a large amount of elements, which can easily exceed 10^4. In this case each global remeshing phase CPU time largely exceed 100 s. Simultaneously the number of remeshing phases increases proportionally with the number of elements. These two combined effects favour the use of

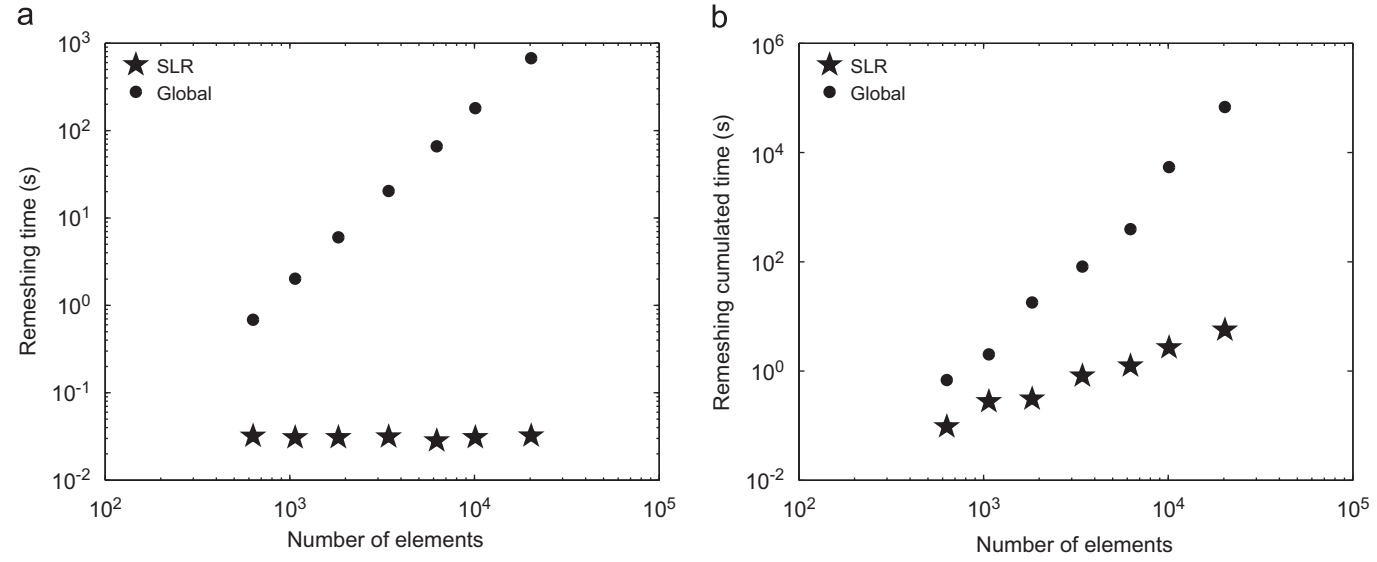

Fig. 5. Loglog plot of the mean CPU time (s) needed to achieve one remeshing phase (a), and of the cumulated CPU time (b) needed by remeshing for the SLR (stars) and global remeshing (filled circles) methods as a function of the number of elements of the model.

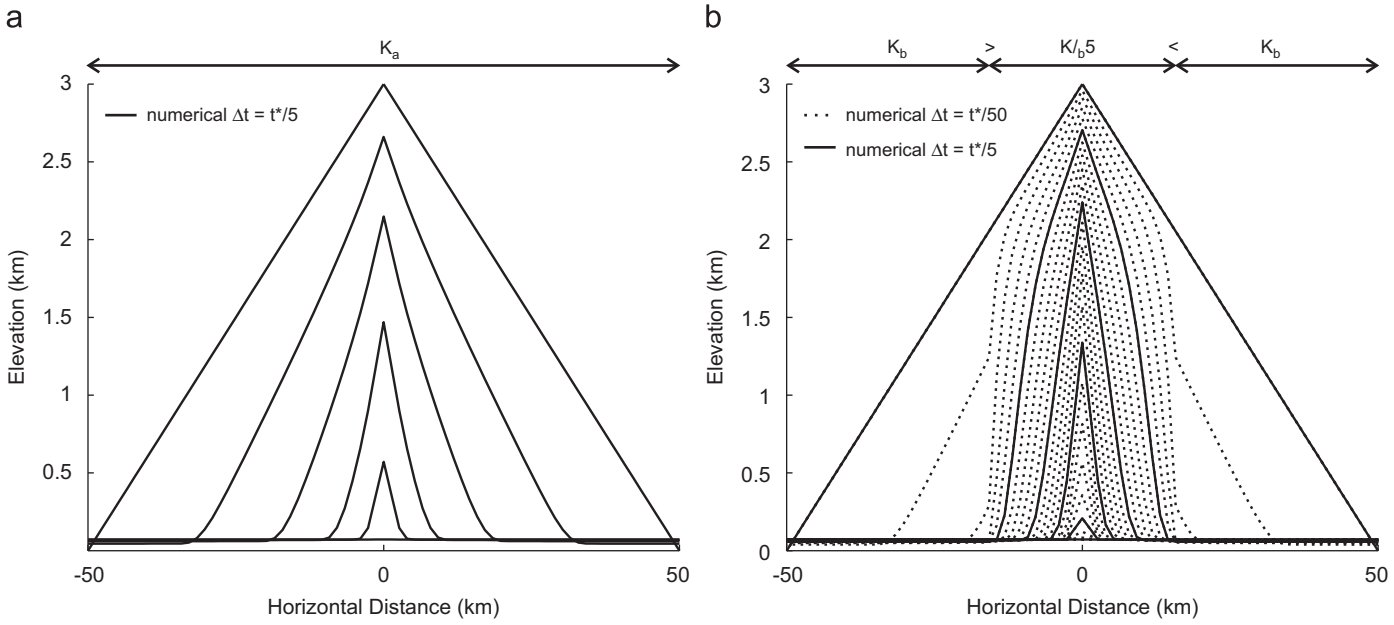

Fig. 6. Time evolution of the surface of the model for erosion by river incision plotted at each 20% ($\Delta t = t_*/5$) of the numerical experiment. (a) Homogeneous erodibility with $K = K_a = 6.4 \times 10^{-10}$ ma$^{0.13}$ s$^{-0.67}$ and the precipitation rate set equal to $P = 1$ m a^{-1}. Experiment (b) presents a spatial contrast of erodibility to river incision, with $K = K_b = 2.15 \times 10^{-9}$ m$^{0.13}$ s$^{-0.67}$ the coefficient of erodibility at the borders of the model being five times greater than at the center. Note the elastic rebound associated with unloading by erosion removal.

the SLR method, which requires only ~ 5 s of cumulated remeshing time for 20 000 elements, while ~ 19 h are needed with global remeshing.

3.4. Remeshing with the dynamic relaxation method

ADELI employs the dynamic relaxation (DR) method for time discretization (Underwood, 1983). As it is an explicit numerical scheme, the associated FEM is conditionally stable Appendix B. Thus we need to check that the errors introduced during remeshing do not lead to numerical divergence. This is likely to occur when the changes in I_r due to each remeshing are cumulated with time. To avoid this accumulation of errors, the time period between each remeshing $\Delta t_{\mathrm{rmesh}}$ must be greater than the numerical relaxation time t_{damp} needed to restore a level of I_r prior remeshing. For instance in the experiment with ~ 6000 elements and for the SLR method t_{damp} is equal to ~ 50 time steps. The evolution of I_r shows a global decrease except between 1000 and 2000 time steps, where $\Delta t_{\mathrm{rmesh}} < t_{\mathrm{damp}}$ (Fig. 4).

Furthermore if we use a visco-elastic rheology instead of the elastic one used in the models presented in this paper, the time between remeshing events needs to be greater than t_{relax} the viscous relaxation time,

$$t_{\mathrm{relax}} = \frac{\min(\mu_{\mathrm{eff}})}{E}, \tag{6}$$

where $\min(\mu_{\mathrm{eff}})$ is the minimum effective viscosity of the medium considered.

4. Application and limitations

4.1. River incision and rock erodibility

To further assess the abilities and limitations of the SLR algorithm, we apply it to model erosion by river incision (Eq. (4)). The set-up of the model is the same as in the previous section. In the two experiments presented here (Fig. 6) the coefficient of bedrock erodibility is either homogeneous or presents an abrupt contrast, i.e. the borders of the mountain are five times more erodible than its center. The SLR algorithm is successful to deal with both and manages to keep constant the number of nodes setting the surface and subsequently the horizontal resolution. Detailed investigations are now required to deepen our understanding of rock erodibility in the interplay between erosion and tectonics.

4.2. Limitations

As a consequence the vertical resolution decreases where the erosion rate exhibits a spatial gradient. Here it happens at the transition zone between high and low erodibility (Fig. 6b).

Another limitation, which is not illustrated here, is the singularity that represents, for the SLR method, a single element forming an acute triangular mountain summit. In our models this singularity mainly occurs if the slope of the surface is greater than 45° on both sides of the mountain summit. In this setting it is impossible for the SLR to remesh the element forming the summit, as all its nodes belong to the surface. However, this singularity can be avoided by swapping the basal face of such a triangular element with its direct neighbour.

When considering surface processes, the main limitation of the SLR algorithm is that it requires to be modified to allow modelling of sedimentation law. For instance we were not able to simulate the sedimentation part of the diffusion law using SLR (Fig. 2). Conversely SLR is not adapted to extensional settings. Both sedimentation and extension would rather require to add nodes where stretching of surface elements is important (small internal angle or large area).

5. Conclusion

Our study has demonstrated the efficiency of the local remeshing algorithm proposed in this paper. Compared to global remeshing, the SLR method is computationally costless, and produces only

localized numerical errors, as interpolation occurs locally on the remeshed elements. Since the nodes of the free surface of the model are preserved throughout the simulation, SLR is an appropriate method in the context of numerical modelling with a particular interest in geomorphology. The SLR is thus a robust remeshing algorithm that enables to simulate erosion over long time scale in FEM modelling. It was successfully applied to study river erosion over an abrupt contrast of rock erodibility.

However, it is not suited for studies with both erosion and sedimentation. The applications of the SLR is not limited to 2*D* models using triangular elements. Its fundamental principles can be easily transposed to 3*D* FEM using tetrahedral elements.

Coupled with DLR, these local remeshing algorithms represent both a prospect for FEM based on Lagrangian formulation and an alternative to ALE and passive markers methods by their abilities to deal with both large deformation and high erosion (e.g., Braun et al., 2008; Fullsack, 1995; Thieulot et al., 2008; Yamato et al., 2007). The coupled SLR–DLR remeshing algorithm has the potential to provide an efficient way to study a wide range of complex geological settings, which require to couple deformation of Earth materials with surface erosion (e.g., Godard et al., 2006; Kaus et al., 2008; Willett, 1999).

Acknowledgements

Thanks to Cédric Thieulot and Boris Kaus for their careful and helpful reviews. We also thank Riad Hassani and Jean Chéry for providing the finite element code, and to Suzanne Pinder for language corrections.

Appendix A. Analytical solutions of erosion laws

Let us consider the elevation of the right side of a triangular mountain belt initially defined as $h(x,t=0)=-(H/l)\,x+H$, where H is the elevation of the summit and l is the horizontal distance between the summit and the foot of the mountain. Analytical evolution of this mountain belt $h(x,t)$ submitted to a slope-dependent erosion law,

$$\frac{\partial h(x,t)}{\partial t}=-K\frac{\partial h(x,t)}{\partial x}, \tag{7}$$

is given by

$$h(x,t)=h(x,t=0)-K\frac{H}{L}t, \tag{8}$$

where K is a coefficient of denudation.

Analytical evolution of the same mountain belt $h(x,t)$ submitted to diffusion of elevation,

$$\frac{\partial h(x,t)}{\partial t}=K\frac{\partial^2 h(x,t)}{\partial x^2}, \tag{9}$$

with the boundary conditions,

$$h(x=l,t)=0, \tag{10}$$

$$\partial h(x=0,t)/\partial x=0, \tag{11}$$

is given by

$$h(x,t)=\int_0^l h(\zeta,0)G(x,t,\zeta)\,d\zeta, \tag{12}$$

where

$$G(x,t,\zeta)=\frac{2}{l}\sum_{n=0}^{l}\cos\left(\frac{\pi(2n+1)}{2l}x\right)\cos\left(\frac{\pi(2n+1)}{2l}\zeta\right)\exp\left(-\frac{K\pi^2(2n+1)^2}{4l^2}t\right), \tag{13}$$

with K the coefficient of diffusion. The numerical integration of Eq. (12) was carried out by means of a trapezoidal rule.

Appendix B. Numerical method

Finite element method deduces the nodal displacement U by solving the force-balance equation which results for long-term geodynamic problems in the following system of simultaneous equations:

$$K_{stiff}U=F_e, \tag{14}$$

where K_{stiff} is the stiffness matrix and F_e the external nodal forces. Two methodologies are commonly used to solve this problem. Implicit methods in which the static system (14) is linearized into a large system of algebraic equation. These methods are computationally expensive. The finite element code ADELI (Hassani et al., 1997) used in this study rather employs Dynamic Relaxation (DR) to solve previous equation (Underwood, 1983). This is an explicit iterative procedure, in which the static system (Eq. (14)) is transferred to an artificial dynamic space by adding artificial inertia and damping forces,

$$M\ddot{U}+C\dot{U}+K_{stiff}U=F_e, \tag{15}$$

where M is a fictious mass matrix chosen in a diagonal form, and C a fictious damping matrix. The steady state solution of this artificial dynamic system (Eq. (15)) is the solution of the static system (Eq. (14)). It is reached when the inertial regularizing term $M\ddot{U}$ is negligible compared to the forces involved in the problem. Inverting previous equation gives an expression of the nodal acceleration,

$$\ddot{U}=M^{-1}(F_e-F_i-C\dot{U}), \tag{16}$$

with $F_i=K_{stiff}U$ the internal nodal forces calculated from the integration of the constitutive law (Eq. (3)). Velocity and displacement are then computed by numerical integration of acceleration.

References

Avouac, J.P., Burov, E.B., 1996. Erosion as a driving mechanism of intracontinental mountain growth. Journal of Geophysical Research 101 (B8), 17747–17769.

Beaumont, C., Fullsack, P., Hamilton, J., 1992. Erosional control of active compressional orogens. In: McClay, K.R. (Ed.), Thrust Tectonics. Chapman & Hall, New York, pp. 1–18.

Beaumont, C., Jamieson, R.A., Nguyen, M.H., Lee, B., 2001. Himalayan tectonics explained by extrusion of a low-viscosity crustal channel coupled to focussed surface denudation. Nature 414, 738–742.

Belytschko, T., Black, T., 1999. Elastic crack growth in finite elements with minimal remeshing. International Journal for Numerical Methods in Engineering 45 (5), 601–620.

Braun, J., Sambridge, M., 1994. Dynamical Lagrangian Remeshing (DLR): a new algorithm for solving large strain deformation problems and its application to fault-propagation folding. Earth and Planetary Science Letters 124, 211–220.

Braun, J., Thieulot, C., Fullsack, P., DeKool, M., Beaumont, C., Huismans, R., 2008. DOUAR: a new three-dimensional creeping flow numerical model for the solution of geological problems. Physics of the Earth and Planetary Interiors 171, 76–91.

Fullsack, P., 1995. An arbitrary Lagrangian–Eulerian formulation for creeping flows and its application in tectonic models. Geophysical Journal International 120 (1), 1–23.

Gilbert, G.K., 1877. Report on the Geology of the Henry Mountains. U.S. Geographical and Geological Survey of the Rocky Mountain Region, Washington, DC, 160pp.

Godard, V., Lavé, J., Cattin, R., 2006. Numerical modelling of erosion processes in the Himalayas of Nepal: effects of spatial variations of rock strength and precipitation. In: Buiter, S.J.H., Schreurs, G. (Eds.), Analogue and Numerical Modelling of Crustal-Scale Processes, Geological Society, vol. 253. Special Publication, London, pp. 341–358.

Godard, V., Cattin, R., Lavé, J., 2009. Erosional control on the dynamics of low-convergence rate continental plateau margins. Geophysical Journal International 179 (2), 763–777.

Hack, J.T., 1957. Studies of longitudinal stream profiles in Virginia and Maryland. U.S. Geological Survey Professional Paper 294-B, 97pp.

Hassani, R., Jongmans, D., Chéry, J., 1997. Study of plate deformation and stress in subduction processes using two-dimensional numerical models. Journal of Geophysical Research 102 (B8), 17951–17965.

Howard, A.D., Kerby, G., 1983. Channel changes in badlands. Geological Society of America Bulletin 94 (6), 739–752.
Howard, A.D., Dietrich, W.E., Seidl, M.A., 1994. Modeling fluvial erosion on regional to continental scales. Journal of Geophysical Research 99 (B7), 13971–13986.
Hwang, C.J., Wu, S.J., 1992. Global and local remeshing algorithms for compressible flows. Journal of Computational Physics 102 (1), 98–113.
Kaus, B.J.P., Steedman, C., Becker, T.W., 2008. From passive continental margin to mountain belt: insights from analytical and numerical models and application to Taiwan. Physics of the Earth and Planetary Interiors 171, 235–251.
Kurfeß, D., Heidbach, O., 2009. CASQUS: A new simulation tool for coupled 3D finite element modeling of tectonic and surface processes based on ABAQUS™and CASCADE. Computers & Geosciences 35 (10), 1959–1967.
Lavé, J., Avouac, J.P., 2001. Fluvial incision and tectonic uplift across the Himalayas of central Nepal. Journal of Geophysical Research 106 (B11), 26561–26591.
Lavé, J., 2005. Analytic solution of the mean elevation of a watershed dominated by fluvial incision and hillslope landslides. Geophysical Research Letters 32 (11), L11403. doi:10.1029/2005GL022482.
Renka, R.J., 1996. ALGORITHM 751. TRIPACK: constrained two-dimensional Delaunay triangulation package. ACM Transactions on Mathematical Software 22 (1), 1–8.
Thieulot, C., Fullsack, P., Braun, J., 2008. Adaptative octree-based finite element analysis of two- and three-dimensional indentation problems. Journal of Geophysical Research 113 (B12), B12207. doi:10.1029/2008JB005591.
Underwood, P., 1983. Dynamic relaxation. In: Hughes, T.J.R., Belytschko, T.B. (Eds.), Computational Methods for Transient Analysis. Elsevier Science Publisher B.V., Netherlands, pp. 245–265.
Willett, S.D., 1999. Orogeny and orography: the effects of erosion on the structure of mountain belts. Journal of Geophysical Research 104 (B12), 28,957–28,981.
Willett, S.D., 2010. Erosion on a line. Tectonophysics 484, 168–180.
Yamato, P., Agard, P., Burov, E., Le Pourhiet, L., Jolivet, L., Tiberi, C., 2007. Burial and exhumation in a subduction wedge: mutual constraints from thermomechanical modeling and natural P-T-t data (Schistes Lustres western Alps). Journal of Geophysical Research 112 (B7), B07410. doi:10.1029/2006JB004441.